Published in final edited form as:
Biochem Biophys Res Commun. 2008 November 28; 376(4): 775–780. doi:10.1016/j.bbrc.2008.09.068.

Generation of a 'Humanized' h*CYP1A1_1A2_Cyp1a1/1a2*(−/−)_*Ahr*^{d} Mouse Line Harboring the Poor-Affinity Aryl Hydrocarbon Receptor

Zhanquan Shi, **Ying Chen**, **Hongbin Dong**, **Robyn M. Amos-Kroohs**, and **Daniel W. Nebert***
*Department of Environmental Health and Center for Environmental Genetics (**CEG**) University of Cincinnati Medical Center, Cincinnati OH 45267-0056*

Abstract

Herein we describe generation of the h*CYP1A1_1A2_Cyp1a1/1a2*(−/−)_*Ahr*^{d} mouse line, which carries human functional *CYP1A1* and *CYP1A2* genes in the absence of mouse *Cyp1a1* and *Cyp1a2* genes, in a (>99.8%) background of the C57BL/6J genome and harboring the poor-affinity aryl hydrocarbon receptor (**AHR**) from the DBA/2J mouse. We have characterized this line by comparing it to our previously created h*CYP1A1_1A2_Cyp1a1/1a2*(−/−)_*Ahr*^{b1} line—which carries the same but has the high-affinity AHR of the C57BL/6J mouse. By quantifying CYP1A1 and CYP1A2 mRNA in liver, lung and kidney of dioxin-treated mice, we show that dose-response curves in h*CYP1A1_1A2_Cyp1a1/1a2*(−/−)_*Ahr*^{d} mice are shifted to the right of those in h*CYP1A1_1A2_Cyp1a1/1a2*(−/−)_*Ahr*^{b1} mice—similar to, but not as robust as, dose-response curves in DBA/2J versus C57BL/6J mice. This new mouse line is perhaps more relevant than the former to human risk assessment vis-à-vis human CYP1A1 and CYP1A2 substrates, because poor-affinity rather than high-affinity AHR occurs in the vast majority of the human population.

Keywords

Cytochrome P450 1 (*CYP1*) genes; humanized mouse line; human risk assessment; CYP1A1 and CYP1A2 substrates; 2,3,7,8-tetrachlorodibenzo-*p*-dioxin (TCDD;dioxin) as a P450 inducer; aryl hydrocarbon receptor (AHR)

INTRODUCTION

Since the 1960s, cytochrome P450 (**CYP**) enzymes were known to be heme-thiolate proteins, localized principally in liver and metabolizing drugs and other foreign chemicals. It is now realized, however, that CYP enzymes are involved in innumerable endogenous functions such as: the metabolism of eicosanoids [1]; biosynthesis of cholesterol and bile acids; steroid synthesis and metabolism; synthesis and degradation of biogenic amines; vitamin D_3 synthesis and metabolism; and hydroxylation of retinoic acid and presumably other morphogens. There are still a few CYP enzymes having unknown functions [2–5].

*To whom correspondence should be addressed: Department of Environmental Health, University of Cincinnati Medical Center, P.O. Box 670056, Cincinnati OH 45267-0056, U.S.A., Tele. 513-558-0373; Fax 513-558-0974; email dan.nebert@uc.edu.

The human and mouse genomes carry 57 and 102 functional *CYP* genes, respectively, with almost all of the additional mouse genes occurring in the *Cyp2*, *Cyp3* and *Cyp4* families; of the 18 mammalian families, *CYP1* has three members in both human and mouse—CYP1A1, CYP1A2 and CYP1B1 [3–6]. Ancestors of the *CYP1A* and *CYP1B* subfamily diverged from one another probably more than 500 million years ago, whereas *CYP1A2* likely arose as a gene duplication event from *CYP1A1* about 450 million years ago. Thus, land animals (including fowl) carry both *CYP1A1* and *CYP1A2*; sea animals do not have the *CYP1A2* gene [2]. The *CYP1A1* and *CYP1A2* genes are located at human chromosome 15q24.1, in head-to-head orientation, 23,306 bases from one transcription start-site to the other [7]. Among three mammalian genomes studied, estimates are that about 10% of gene duplication pairs share bidirectional promoters [8].

Human/rodent CYP1A2 orthologs are well known to exhibit species-specific differences in the rates by which various substrates are metabolized [9]. For example, human and mouse CYP1A2 differ by 3- to 7-fold in ethoxyresorufin *O*-deethylation [10] and uroporphyrinogen oxidation [11]. Drug or carcinogen metabolism can differ in the rodent, and extrapolation of rodent data to human populations is thus prone to error; therefore, one of the long-term goals of this laboratory has been to insert human metabolism gene(s) in place of mouse orthologous gene(s).

Cyp1a1(−/−) [12] and *Cyp1a2*(−/−) [13] single-knockout and the *Cyp1a1/1a2*(−/−) double-knockout [14] mouse lines have been created. Insertion of a bacterial artificial chromosome (**BAC**) containing the human *CYP1A1_CYP1A2* locus—including 56 kb 3′-ward of *CYP1A1* and 86 kb 3′-ward of *CYP1A2* [7;15;16]—resulted in the successful generation of "humanized" h*CYP1A1_1A2_Cyp1a1*(−/−) and h*CYP1A1_1A2_Cyp1a2*(−/−) lines, which contain both human *CYP1A1* and *CYP1A2* genes in the absence of either the mouse *Cyp1a1* or *Cyp1a2* ortholog, respectively. These lines have been used for theophylline [15] and the food mutagen 2-amino-1-methyl-6-phenylimidazo[4,5-*b*]pyridine (**PhIP**) [16;17]. In the first two instances [15;16], human hepatic CYP1A2 was demonstrated to be responsible for the "human metabolite profile" in the absence of mouse CYP1A2; in the third case [17], human lung CYP1A1 was shown to be accountable for the human PhIP metabolite profile when the mouse *Cyp1a1* gene was lacking.

Studying the h*CYP1A1_1A2_Cyp1a1*(−/−) and h*CYP1A1_1A2_Cyp1a2*(−/−) lines separately, however, is cumbersome. For human risk assessment of CYP1A1 or CYP1A2 substrates, it would be preferable to have a mouse line carrying both human *CYP1A1* and *CYP1A2* genes in the absence of both mouse orthologs. We therefore generated the h*CYP1A1_1A2_Cyp1a1/1a2*(−/−)_*Ahr*^{b1} mouse line [14]; this line has functional human *CYP1A1* and *CYP1A2* genes, in the absence of both mouse *Cyp1a1* and *Cyp1a2* genes, and is on a theoretically >99.8% C57BL/6J (**B6**) genetic background [14]. Because this line expresses the B6 high-affinity AHR encoded by the *Ahr*^{b1} allele, however, there is still some concern—because the vast majority of humans (*i.e.* >90–95%) carries the poor-affinity receptor, which is closer in function to that of the DBA/2J (**D2**) mouse harboring the *Ahr*^{d} allele [6]. Hence, we have now developed a humanized line containing the homozygous *Ahr*$^{d/d}$ genotype. Characterization of this new line is the focus of the present report.

MATERIALS AND METHODS

Mice

C57BL/6J (**B6**) and DBA/2J (**D2**) inbred mouse strains and the B6.D2-*Ahr*^{d} congenic line were purchased from The Jackson Laboratory (Bar Harbor, ME). Characterization of the humanized h*CYP1A1_1A2_Cyp1a1/1a2*(−/−)_*Ahr*$^{\boldsymbol{b1}}$ mouse line, which has >99.8% C57BL/6J genetic background harboring the *Ahr*^{b1} allele, has been reported; this line has a single copy of the

BAC containing the human *CYP1A1_CYP1A2* locus, inserted randomly into the genome [14]. In the present study—the new humanized h*CYP1A1_1A2_Cyp1a1/1a2*(−/−)_*Ahr*^{d} mouse line is also on a >99.8% C57BL/6J genetic background, except it is harboring the *Ahr*^{d} allele. This line was developed by breeding h*CYP1A1_1A2_Cyp1a1/1a2*(−/−)_*Ahr*^{b1} with B6.D2-Ahr^{d} mice. All experiments involving these mice were conducted in accordance with the National Institutes of Health (**NIH**) standards for the care and use of experimental animals and the University Cincinnati Institutional Animal Care and Use Committee.

Genotyping mice by PCR

Crude genomic DNA for genotyping was prepared from a 4-mm tail biopsy using the DirectPCR lysis reagent according to the manufacturer's protocol (Viagen Biotech Inc.; Los Angeles, CA). PCR primers used to detect individual alleles are summarized in Table 1. The *Ahr*^{b1} and Ahr^{d} alleles were detected using the same primer pair—with a 300-bp product representing the *Ahr*^{b1} allele and a 260-bp product representing the *Ahr*^{d} allele.

Treatment of the mice

For all four genotype groups, female mice (age 2–3 months) were treated with 2,3,7,8-tetrachlorodibenzo-*p*-dioxin (**TCDD**) intraperitoneally at a single dose of 0.1, 1.0, 10 or 100 μg/kg, respectively; the vehicle only (corn oil) was used for the untreated groups (0 μg/kg). Mice were sacrificed 48 h later.

Biohazard precaution

TCDD is highly toxic and a presumed human carcinogen. All personnel were instructed in safe handling procedures. Lab coats, gloves and masks were worn at all times, and contaminated materials were collected separately for disposal by the Hazardous Waste Unit or by independent contractors. TCDD-treated mice were housed separately, and their carcasses regarded as contaminated biological materials.

Reverse transcription and quantitative real-time polymerase chain reaction (qRT-PCR)

Mouse tissues were harvested and frozen in liquid nitrogen, and stored at ™80°C until use. Total RNA was isolated using Tri Reagent (Molecular Research Center, Inc.; Cincinnati, OH). First-strand cDNA was synthesized from 1 μg of total RNA with Verso™ cDNA kit (Thermal Fisher Scientific Inc.; Waltham, MA). Reaction mixtures of 20 μl containing 125 nM gene-specific primer sets, 1 μl of cDNA template, and 10 μl of iQ™SYBR Green Supermix (Bio-Rad) was used for qRT-PCR in a DNA Engine Opticon-2 Real Time PCR Detection System (MJ Research; Waltham, MA), and results were analyzed using the software provided by the manufacturer. Primers used in qRT-PCR are summarized in Table 1. For each examined tissue, individual TCDD-induced mRNA levels are reported as the fold increase over that by β-actin (**ACTB**) mRNA. Thus, one can compare the relative mRNA levels within a tissue, but not between tissues. The cycle numbers for the detection of ACTB mRNA did not differ significantly between untreated and treated groups.

Statistical analyses

Statistics were performed using SigmaStat Statistical Analysis software (SPSS Inc.; Chicago, IL). Group means of the cycle difference ($\Delta \boldsymbol{C_t}$) after normalization of ACTB mRNA were compared by one-way ANOVA, followed by the Tukey Post-hoc test for pairwise comparison-of-means. All data were normally distributed and reported as the means ± S.E. *P*-values of <0.05 are considered as statistically significant.

RESULTS AND DISCUSSION

Generation of the hCYP1A1_1A2_Cyp1a1/1a2(−/−)_Ahr^d mouse line

Given the fact that human poor-affinity AHR resembles more closely poor-affinity AHR of D2 mice, we developed a humanized line containing the *Ahr^d* allele. This was achieved by mating h*CYP1A1_1A2_Cyp1a1/1a2*(−/−)*_Ahr^{b1}* mice with B6.D2-*Ahr^d* congenic mice (Fig. 1). Historically, congenic lines were developed by George Snell in the 1940s, with the idea to place the major histocompatibility complex (*H2*) of one inbred mouse into the genome of a second type of mouse; graft-versus-host diseases could thus be studied—as related to the *H2* locus and in the absence of modifying genes located in *trans*. To develop a congenic line that contains a >99.8% homogeneous genetic background, a selected genotype (or phenotype) from one inbred strain must be backcrossed 20 generations into another inbred strain.

The B6.D2-*Ahr^d* congenic line carries the *Ahr^d* locus (and unknown amounts of adjacent DNA from the D2 mouse on chromosome 12), on a theoretically >99.8% B6 genetic background [18]. Intercrossing of h*CYP1A1_1A2*(+/−)*_Cyp1a1/1a2*(+/−)*_Ahr(b1/d)* heterozygotes (Fig. 1) thus gave rise to the h*CYP1A1_1A2(+/+)_Cyp1a1/1a2*(−/−)*_Ahr(d/d)* homozygous line, which basically differs from our previous humanized line only at the *Ahr* locus.

Homozygous h*CYP1A1_1A2_Cyp1a1/1a2*(−/−)*_Ahr^d* offspring are healthy, fertile and exhibit a normal Mendelian frequency—indistinguishable from the h*CYP1A1_1A2_Cyp1a1/1a2*(−/−)*_Ahr^{b1}* line (not shown). Both of these humanized mouse lines carry human functional *CYP1A1* and *CYP1A2* genes replacing the mouse orthologs. The two human genes are regulated by the endogenous mouse AHR: high-affinity AHR in the h*CYP1A1_1A2_Cyp1a1/1a2*(−/−)*_Ahr^{b1}* line [14], versus poor-affinity AHR in the h*CYP1A1_1A2_Cyp1a1/1a2*(−/−)*_Ahr^d* line. To initially characterize this newly created humanized mouse line, we compared the induction profiles of human versus mouse CYP1A1 and CYP1A2 mRNA in selected tissues, using a wide range of TCDD doses. This experimental approach had originally been carried out, examining the induction of aryl hydrocarbon hydroxylase (**CYP1A1**) activity in liver of TCDD-treated B6 and D2 mice; from the 10- to 15-fold shift-to-the-right in the dose-response curves between B6 and D2, a receptor was hypothesized to explain these findings [19].

Induction of human CYP1A1

In h*CYP1A1_1A2_Cyp1a1/1a2*(−/−)*_Ahr^{b1}* mice containing the high-affinity AHR (Fig. 2A), human CYP1A1 mRNA levels became elevated already at the 0.1 μg/kg dose of TCDD and accumulated in a dose-dependent manner reaching ~250-, ~40- and ~500-fold induction in liver, lung and kidney, respectively, at the highest TCDD dose. In these same tissues of the h*CYP1A1_1A2_Cyp1a1/1a2*(−/−)*_Ahr^d* mouse carrying the poor-affinity AHR, the dose-response curve was shifted-to-the-right ~3- to 4-fold: human CYP1A1 mRNA induction was not significantly detectable until TCDD doses of 1.0 μg/kg or higher and the highest accumulated induction levels were ~150-, ~56- and ~130-fold in liver, lung and kidney, respectively. Whereas human CYP1A1 mRNA amounts in both lines were not significantly different in liver at the 10 μg/kg dose of TCDD, the mRNA levels were significantly greater at the other doses in liver and at all doses in lung and kidney of h*CYP1A1_1A2_Cyp1a1/1a2*(−/−)*_Ahr^{b1}*, compared with those of h*CYP1A1_1A2_Cyp1a1/1a2*(−/−)*_Ahr^d* mice. In either humanized line, as expected, mouse CYP1A1 mRNA was undetectable (not shown).

Induction of mouse CYP1A1

Using the same induction regimen, we also studied the mouse CYP1A1 mRNA in B6 (high-affinity-AHR) and D2 (poor-affinity-AHR) mice (Fig. 2B). In all three tissues, the B6 *Cyp1a1* gene responded more robustly to TCDD, when compared with the human *CYP1A1*

gene under the control of the same mouse AHR. Mouse CYP1A1 mRNA also showed dose-dependent responses at all four TCDD doses.

In B6 animals (Fig. 2B), mouse CYP1A1 mRNA levels were strikingly elevated already at the 0.1 μg/kg dose of TCDD and accumulated in a dose-dependent manner reaching ~6100-, ~66- and ~2000-fold induction in liver, lung and kidney, respectively, at the highest TCDD dose. In these same tissues of the D2 mouse, the dose-response curve was shifted ~10- to 12-fold to the right; the highest accumulated induction levels of mouse CYP1A1 mRNA were ~5200-, ~1400- and ~390-fold in liver, lung and kidney, respectively. Note that B6 lung basal CYP1A1 mRNA amounts are ~16-fold greater than that in D2.

Induction of human CYP1A2

In TCDD-treated h*CYP1A1_1A2_Cyp1a1/1a2*(−/−)_*Ahr*^{b1} mice (Fig. 3A), human CYP1A2 mRNA levels were increased in a dose-dependent manner (at all four TCDD doses) in liver, reaching ~140-fold maximal induction over basal levels; in lung, maximal induction of ~12-fold was accomplished at the 1.0 μg/kg TCDD dose; in kidney, accumulation of human CYP1A2 mRNA occurred at doses of only 1.0 μg/kg and higher, with maximal induction of ~14-fold over basal levels. In TCDD-treated h*CYP1A1_1A2_Cyp1a1/1a2*(−/−)_*Ahr*^{d} mice, human CYP1A2 mRNA in liver was maximally induced ~37-fold at the 10 μg/kg TCDD dose; in lung maximal increases of ~3.5-fold occurred at the 1 μg/kg dose; in kidney maximal induction of ~10-fold were seen at the 100 μg/kg dose. While evidence of a shift-to-the-right in the dose-response curves was seen in lung and kidney, in liver any differences in accumulated human CYP1A2 mRNA between the two humanized lines were found only at the 0.1 and 100 μg/kg doses. Although extremely low, human CYP1A2 basal levels in the kidney were ~5 times greater in h*CYP1A1_1A2_Cyp1a1/1a2*(−/−)_*Ahr*^{b1} mice than in h*CYP1A1_1A2_Cyp1a1/1a2*(−/−)_*Ahr*^{d} mice. In either humanized line, as expected, mouse CYP1A2 mRNA was undetectable (not shown).

Induction of mouse CYP1A2

We also examined mouse *Cyp1a2* gene expression in these three tissues (Fig. 3B). Mouse CYP1A2 mRNA from B6 liver revealed a dose-dependent response at doses from 0.1 to 10 μg/kg of TCDD, with maximal increases of ~100-fold. In lung and kidney dose-dependent responses were also found—with maximal induction of ~75- and 100-fold, respectively, reached at the 100 μg/kg TCDD dose. In B6 lung, mouse CYP1A2 mRNA amounts were no different at 0.1, 1.0 and 10 μg/kg doses of TCDD.

In liver and lung of the D2 mouse, the dose-response curve was shifted-to-the-right ~10- to 15-fold (Fig. 3B), whereas B6-D2 differences in kidney were apparent only at the 0.1 and 100 μg/kg doses of TCDD; the highest accumulated induction levels of mouse CYP1A2 mRNA were ~56-, ~50- and ~14-fold in liver, lung and kidney, respectively.

Absolute CYP1A1 and CYP1A2 mRNA levels in humanized lines versus B6 mouse

It is known that mammalian CYP1A1 basal mRNA is negligible, resulting in no detectable CYP1A1 protein in virtually any tissue, whereas basal levels of CYP1A2 mRNA and protein are relatively high in liver; induction by TCDD increases these levels, but—due to negligible basal levels—"fold-induction" is generally not a useful parameter [6;20]. In the present study, we found that mouse CYP1A1 maximally induced mRNA concentrations were roughly 10 times higher than human CYP1A1 in liver and lung and 100-fold greater in kidney (Fig. 2). In contrast, mouse CYP1A2 maximally induced mRNA levels were <2-fold higher than human CYP1A2 in liver, but ~7-fold greater in lung, and ~9-fold higher in kidney (Fig. 3).

Human maximally induced CYP1A2 in liver was ~12 times higher than human maximally induced CYP1A1 mRNA, whereas mouse maximally induced CYP1A2 in liver was ~3-fold greater than mouse maximally induced CYP1A1 mRNA. Human maximally induced CYP1A1 levels in lung and kidney were both ~7-fold greater than human maximally induced CYP1A2 mRNA, whereas mouse maximally induced CYP1A1 in lung and kidney was ~13- and ~96-fold higher than mouse maximally induced CYP1A2 mRNA.

How representative are these humanized *CYP1A* mouse lines to individuals in a human population? Clearly, it is possible that the individual from whom the BAC library was derived [7] might represent an "outlier" as far as CYP1A1 and CYP1A2 expression.

In both lung and kidney, maximally induced expression of human CYP1A2 mRNA seen in the humanized lines and mouse CYP1A2 mRNA seen in the B6 mouse is quite low (~0.01-fold of ACTB mRNA); therefore, these levels are negligible—and no CYP1A2 protein is usually detected on Western immunoblots of these tissues. Maximally induced expression of human CYP1A1 mRNA in kidney shows much lower levels (~1%) than maximally induced expression of mouse CYP1A1 mRNA seen in B6 kidney. These findings call into question how important human CYP1A-dependent metabolism might be in both lung and kidney of these two humanized mouse lines. Alternatively, it is possible that the 180-kb BAC containing the human *CYP1A1* and *CYP1A2* genes [7] does not include all of the *cis* and/or *trans* regulatory sites needed for "normal" expression of these two transgenes in mouse lung and kidney. In addition, lung and kidney (more so than liver) are organs comprised of numerous heterogeneous cell types; qRT-PCR is so sensitive that it might detect CYP1A1 or CYP1A2 mRNA at quite high levels in one cell type that represents a minute amount of the entire organ. One might be able to resolve these questions by determining precise copy numbers of CYP1A1 and CYP1A2 mRNA in the various humanized *CYP1A* mouse lines, as well as in established tissue culture lines that are derived from human versus mouse specific cell types.

Conclusions

By breeding h*CYP1A1_1A2_Cyp1a1/1a2*(−/−)_*Ahr*^{b1} mice with B6.D2-*Ahr*^{d} congenic mice, we generated the humanized h*CYP1A1_1A2_Cyp1a1/1a2*(−/−)_*Ahr*^{d} line, which carries the human *CYP1A1* and *CYP1A2* genes in the absence of the mouse *Cyp1a1* and *Cyp1a2* orthologs. Human *CYP1A1* and *CYP1A2* are controlled by the endogenous mouse high-affinity AHR in the h*CYP1A1_1A2_Cyp1a1/1a2*(−/−)_*Ahr*^{b1} line, and by the endogenous mouse poor-affinity AHR in the h*CYP1A1_1A2_Cyp1a1/1a2*(−/−)_*Ahr*^{d} line. We have characterized both humanized lines by quantifying human CYP1A mRNA levels in liver, lung and kidney—as a function of four doses of the potent inducer, dioxin. We have compared dose-response curves of those human mRNA levels with those of mouse CYP1A mRNA levels in B6 (high-affinity) versus D2 (poor-affinity) mice. Although subtle differences exist, the shift-to-the-right in dose-response curves can be visualized in all three organs between the h*CYP1A1_1A2_Cyp1a1/1a2*(−/−)_*Ahr*^{b1} and h*CYP1A1_1A2_Cyp1a1/1a2*(−/−)_*Ahr*^{d} lines, and more robustly in the three organs between the B6 and D2 inbred strains.

We believe this newly-developed h*CYP1A1_1A2_Cyp1a1/1a2*(−/−)_*Ahr*^{d} line will complement the previously described h*CYP1A1_1A2_Cyp1a1/1a2*(−/−)_*Ahr*^{b1} line, in carrying out pharmacokinetic and human risk assessment studies—involving any drug or environmental toxicant that is an effective substrate for CYP1A1 or CYP1A2. Researchers should now be able to compare the poor-affinity-AHR line with the high-affinity-AHR line, with regard to varying doses of environmental toxicants and/or drugs. Upon publication of this report, this line will be made commercially available by The Jackson Laboratories (Bar Harbor, Maine).

Acknowledgements

We thank our colleagues for many fruitful discussions and careful readings of this manuscript. We appreciate the success by Drs. Shige Uno and Tim Dalton in generating the original *Cyp1a1/1a2*(−/−) double-knockout genotype, from which the present humanized line was subsequently possible. Supported, in part, by NIH Grants R01 ES014403 (D.W.N.) and P30 ES06096 (D.W.N.).

References

1. Nebert DW, Karp CL. Endogenous functions of the aryl hydrocarbon receptor: intersection of cytochrome P450 (CYP)1-metabolized eicosanoids and AHR biology. J Biol Chem 2008;283in press
2. Nelson DR, Koymans L, Kamataki T, Stegeman JJ, Feyereisen R, Waxman DJ, Waterman MR, Gotoh O, Coon MJ, Estabrook RW, Gunsalus IC, Nebert DW. P450 superfamily: update on new sequences, gene mapping, accession numbers and nomenclature. Pharmacogenetics 1996;6:1–42. [PubMed: 8845856]
3. Nelson DR, Zeldin DC, Hoffman SM, Maltais LJ, Wain HM, Nebert DW. Comparison of cytochrome P450 (*CYP*) genes from the mouse and human genomes, including nomenclature recommendations for genes, pseudogenes and alternative-splice variants. Pharmacogenetics 2004;14:1–18. [PubMed: 15128046]
4. Nebert DW, Dalton TP. The role of cytochrome P450 enzymes in endogenous signalling pathways and environmental carcinogenesis. Nat Rev Cancer 2006;6:947–960. [PubMed: 17128211]
5. Stark K, Guengerich FP. Characterization of orphan human cytochromes P450. Drug Metab Rev 2007;39:627–637. [PubMed: 17786643]
6. Nebert DW, Dalton TP, Okey AB, Gonzalez FJ. Role of aryl hydrocarbon receptor-mediated induction of the CYP1 enzymes in environmental toxicity and cancer. J Biol Chem 2004;279:23847–23850. [PubMed: 15028720]
7. Jiang Z, Dalton TP, Jin L, Wang B, Tsuneoka Y, Shertzer HG, Deka R, Nebert DW. Toward the evaluation of function in genetic variability: characterizing human SNP frequencies and establishing BAC-transgenic mice carrying the human *CYP1A1_CYP1A2* locus. Hum Mutat 2005;25:196–206. [PubMed: 15643613]
8. Li YY, Yu H, Guo ZM, Guo TQ, Tu K, Li YX. Systematic analysis of head-to-head gene organization: evolutionary conservation and potential biological relevance. PLoS Comput Biol 2006;2:e74. [PubMed: 16839196]
9. Turesky RJ. Interspecies metabolism of heterocyclic aromatic amines and the uncertainties in extrapolation of animal toxicity data for human risk assessment. Mol Nutr Food Res 2005;49:101–117. [PubMed: 15617087]
10. Aoyama T, Gonzalez FJ, Gelboin HV. Human cDNA-expressed cytochrome P450 IA2: mutagen activation and substrate specificity. Mol Carcinog 1989;2:192–198. [PubMed: 2803520]
11. Nichols RC, Cooper S, Trask HW, Gorman N, Dalton TP, Nebert DW, Sinclair JF, Sinclair PR. Uroporphyrin accumulation in hepatoma cells expressing human or mouse CYP1A2: relation to the role of CYP1A2 in human porphyria cutanea tarda. Biochem Pharmacol 2003;65:545–550. [PubMed: 12566081]
12. Dalton TP, Dieter MZ, Matlib RS, Childs NL, Shertzer HG, Genter MB, Nebert DW. Targeted knockout of *Cyp1a1* gene does not alter hepatic constitutive expression of other genes in the mouse [*Ah*] battery. Biochem Biophys Res Commun 2000;267:184–189. [PubMed: 10623596]
13. Liang HC, Li H, McKinnon RA, Duffy JJ, Potter SS, Puga A, Nebert DW. *Cyp1a2*(−/−) null mutant mice develop normally but show deficient drug metabolism. Proc Natl Acad Sci USA 1996;93:1671–1676. [PubMed: 8643688]
14. Dragin N, Uno S, Wang B, Dalton TP, Nebert DW. Generation of a 'humanized' h*CYP1A1_1A2_Cyp1a1/1a2*(−/−) mouse line. Biochem Biophys Res Commun 2007;359:635–642. [PubMed: 17560947]
15. Derkenne S, Curran CP, Shertzer HG, Dalton TP, Dragin N, Nebert DW. Theophylline pharmacokinetics: comparison of *Cyp1a1*(−/−) and *Cyp1a2*(−/−) knockout mice, humanized *hCYP1A1_1A2* knock-in mice lacking either the mouse *Cyp1a1* or *Cyp1a2* gene, and *Cyp1(+/+)* wild-type mice. Pharmacogenet Genomics 2005;15:503–511. [PubMed: 15970798]

16. Cheung C, Ma X, Krausz KW, Kimura S, Feigenbaum L, Dalton TP, Nebert DW, Idle JR, Gonzalez FJ. Differential metabolism of 2-amino-1-methyl-6-phenylimidazo[4,5-*b*]pyridine (PhIP) in mice humanized for *CYP1A1* and *CYP1A2*. Chem Res Toxicol 2005;18:1471–1478. [PubMed: 16167840]
17. Ma X, Idle JR, Malfatti MA, Krausz KW, Nebert DW, Chen CS, Felton JS, Waxman DJ, Gonzalez FJ. Mouse lung CYP1A1 catalyzes the metabolic activation of 2-amino-1-methyl-6-phenylimidazo [4,5-*b*]pyridine (PhIP). Carcinogenesis 2007;28:732–737. [PubMed: 17052995]
18. Nebert DW. Pharmacogenetics: An approach to understanding chemical and biologic aspects of cancer. J Natl Cancer Inst 1980;64:1279–1290. [PubMed: 6929368]
19. Poland AP, Glover E, Robinson JR, Nebert DW. Genetic expression of aryl hydrocarbon hydroxylase activity: induction of monooxygenase activities and cytochrome P_1-450 formation by 2,3,7,8-tetrachlorodibenzo-*p*-dioxin in mice genetically “nonresponsive” to other aromatic hydrocarbons. J Biol Chem 1974;249:5599–5606. [PubMed: 4370044]
20. Eaton DL, Gallagher EP, Bammler TK, Kunze KL. Role of cytochrome P450 1A2 in chemical carcinogenesis: implications for human variability in expression and enzyme activity. Pharmacogenetics 1995;5:259–274. [PubMed: 8563766]

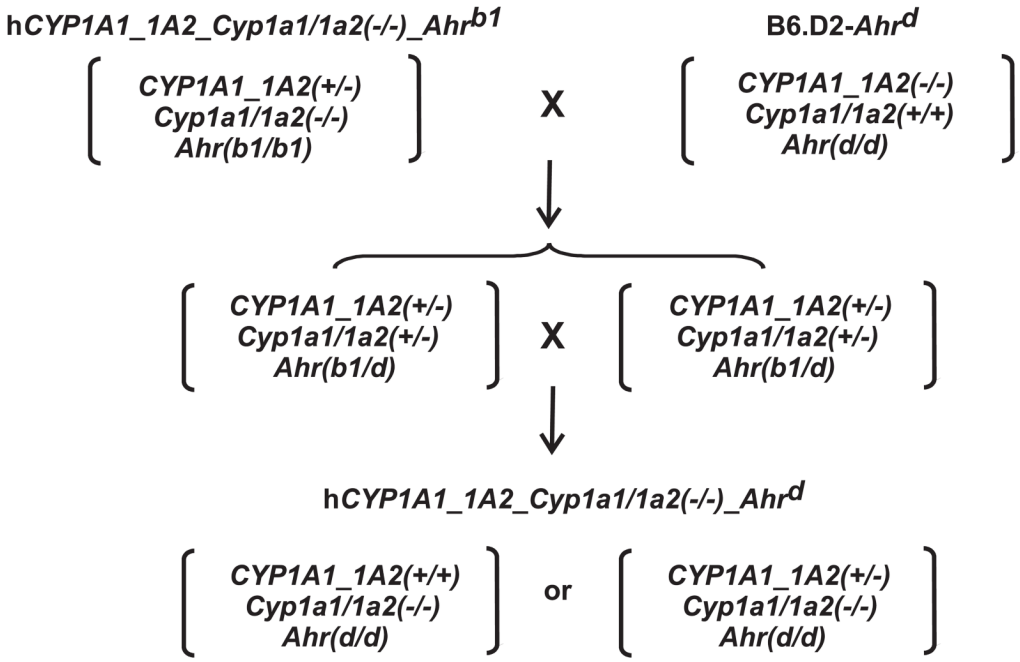

FIG. 1.

Breeding scheme to generate the h*CYP1A1_CYP1A2_Cyp1a1/1a2*(−/−)-*Ahr*^{d} (***Ahr*^{d}**) mouse line. The h*CYP1A1_CYP1A2_Cyp1a1/1a2*(−/−)-*Ahr*^{b1} mice were crossed with B6.D2-*Ahr*^{d} congenic mice to produce heterozygotes, following which homozygous humanized mice harboring two *Ahr*^{d} alleles on a >99.8% C57BL/6J genetic background were created. Homozygotes for the h*CYP1A1_1A2* insertion can be generated one-fourth of the time by mating two heterozygotes, but we cannot distinguish heterozygotes from homozygotes by our current PCR genotyping, because the region of chromosomal insertion is unknown. The only way to distinguish between these two would be to measure the copy number of the h*CYP1A1_1A2* genes. Consequently, the data from both h*CYP1A1_1A2* lines represent a mixture of heterozygotes and homozygotes at the h*CYP1A1_CYP1A2* locus.

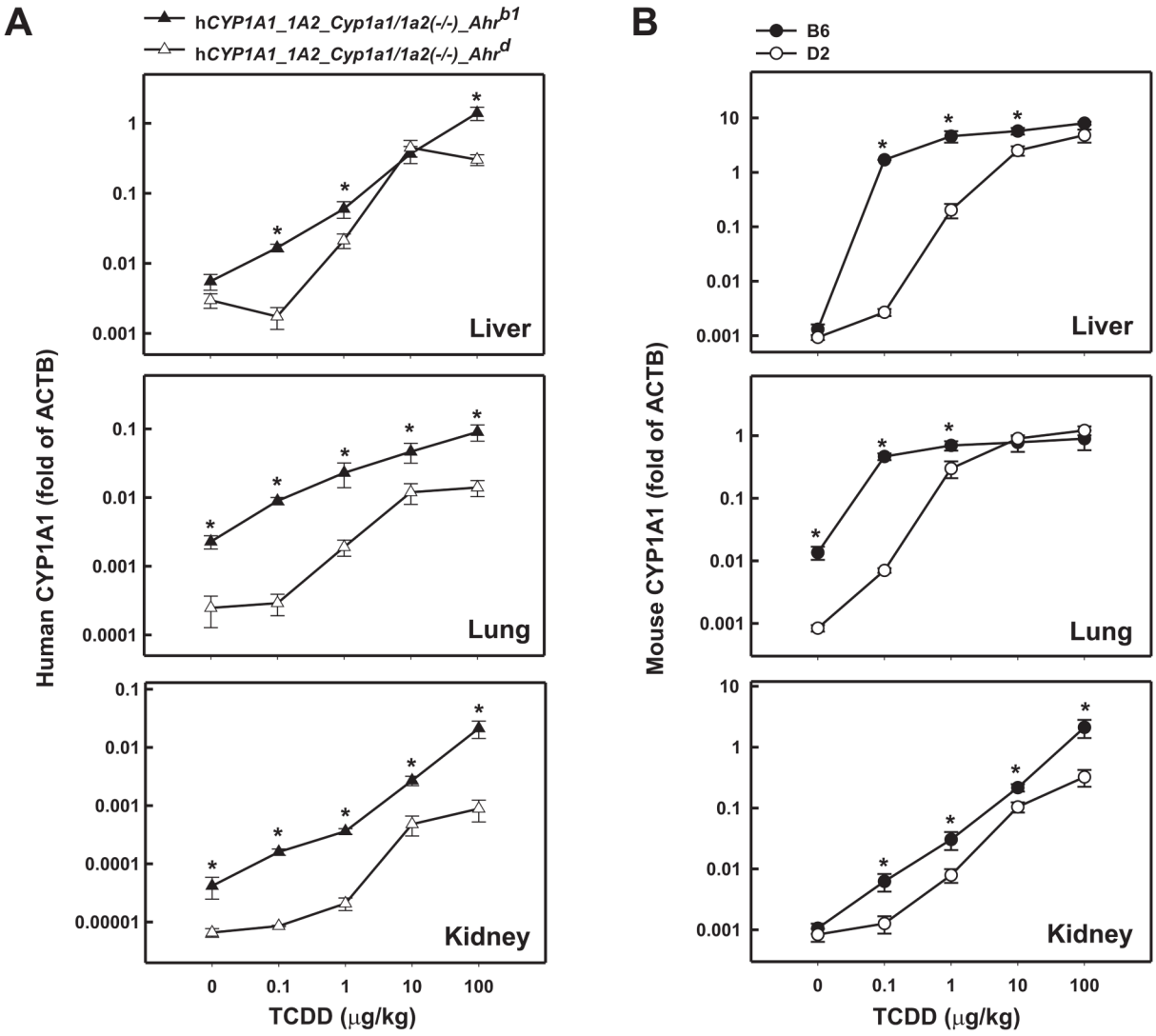

FIG. 2.

Log-log dose-response plots of CYP1A1 mRNA as a function of administered TCDD in liver, lung and kidney. Mice received either vehicle only or one of four doses of intraperitoneal TCDD 48 h before killing. Human (***A***) and mouse (***B***) CYP1A1 mRNA levels were compared by normalizing their concentrations to that of β-actin (**ACTB**) mRNA; PCR reactions for CYP1A1 mRNA and ACTB mRNA were performed on the same plate. Based on the plate reader, the efficiency for each single well was >90%. Note the striking differences in values on the ordinates. Data are reported as means ± S.E.M. (N=3–4 mice per group). ***P* <0.05, when comparing mRNA levels for that gene, at the same dose of TCDD, between the two mouse lines (***A***) or between the two inbred strains (***B***).

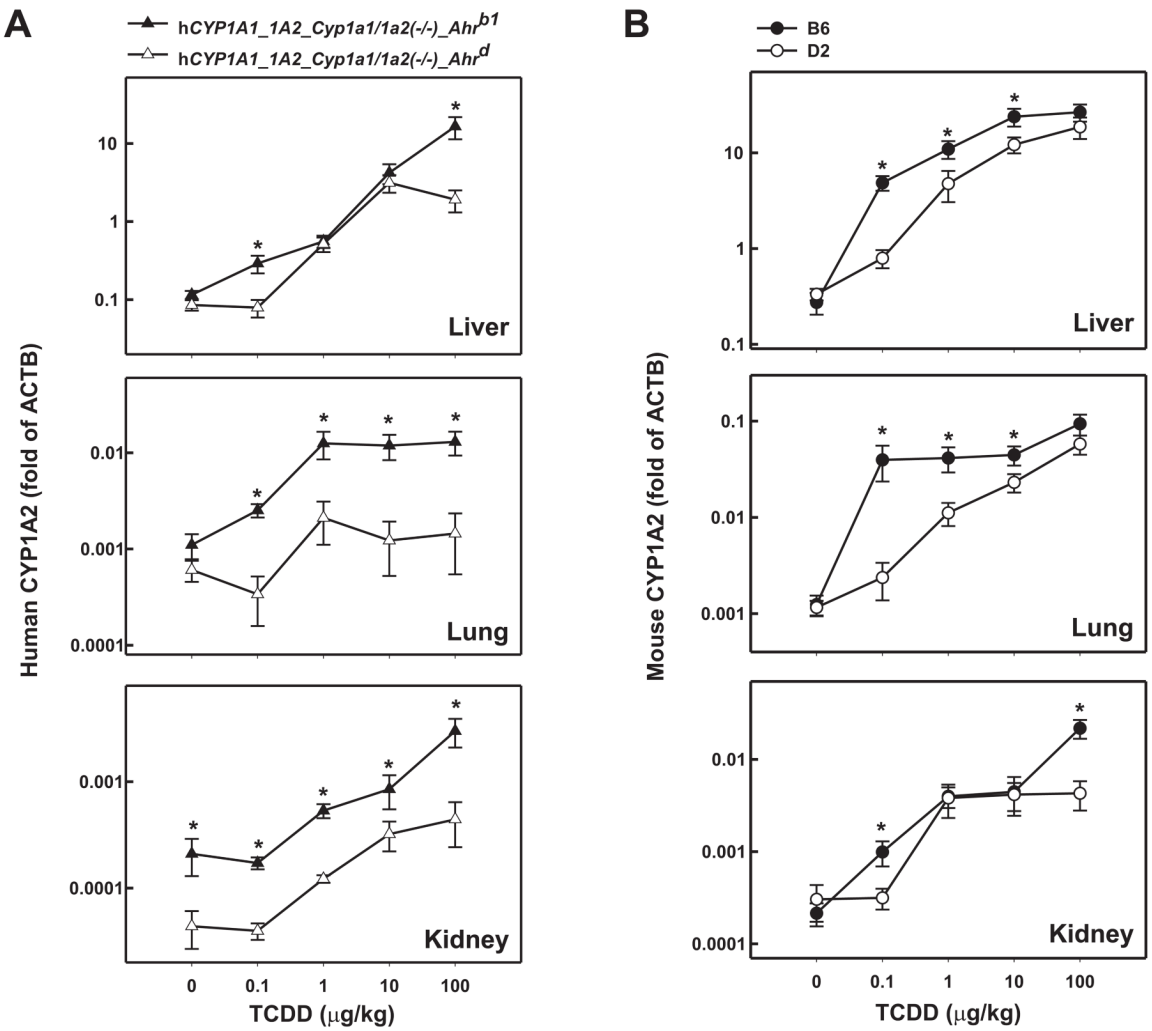

FIG. 3.

Log-log dose-response plots of CYP1A2 mRNA as a function of administered TCDD in liver, lung and kidney from the same mice as shown in Fig. 2. Human (***A***) and mouse (***B***) CYP1A2 mRNA levels were measured identically to that described in the Fig. 2 legend. ***P* <0.05, when comparing mRNA levels for that gene, at the same dose of TCDD, between the two mouse lines (***A***) or between the two inbred strains (***B***).

Table 1

Primer pairs used in genotyping and in qRT-PCR

Genotyping		
Allele	**Forward**	**Reverse**
h*CYP1A1(+)*	5′-GCAGCCCTGTTTGTTCCTG-3′	5′-AGGCTGGCCTATGTGGTCTA-3′
h*CYP1A2(+)*	5′-AGGATTGGCATTGTTGAAGG-3′	5′-GGGCACTGGCCATAGTATTC-3′
***Cyp1a1/1a2*(−/−)**	5′-GTCAAAGTAACCAGACACATCCTGC-3′	5′-GACATAGGAGCTACCTACAC-3′
Cyp1a1(+)	5′-CTGTCTCTGAATCTTACTGCAGCC-3′	5′-GGGCATAGAGCAGGACAGAGCTT-3′
***Cyp1a1*(−)**	5′-CTGTCTCTGAATCTTACTGCAGCC-3′	5′-GTCAAAGTAACCAGACACATCCTG C-3′
Ahr(b1)* or *Ahr(d)	5′-CAGTGGGAATAAGGCAAGAGTGA-3′	5′-AGGGAGATGAAGTATGTGTATGTA-3′
qRT-PCR		
MRNA	**Forward**	**Reverse**
Human CYP1A1	5′-CACTTCCGCTTGCCCATG-3′	5′-ACAACAAGAGACACAAGTTTG-3′
Human CYP1A2	5′-CACAACAAGGGACACAACG-3′	5′-CTTGCCCATGCCAAACAGC-3′
Mouse CYP1A1	5′-CAGACCTCAGCTGCCCTATC-3′	5′-CTTGCCCAAACCAAAGAGAG-3′
Mouse CYP1A2	5′-AAGACAATGGCGGTCTCATC-3′	5′-GACGGTCAGAAAGCCGTGGT-3′
Mouse β-actin	5′-CATCCGTAAAGACCTCTATGCC-3′	5′-ACGCAGCTCAGTAACAGTCC-3′